Renewable Energy 252 (2025) 123500



Contents lists available at ScienceDirect

Renewable Energy

journal homepage: www.elsevier.com/locate/renene

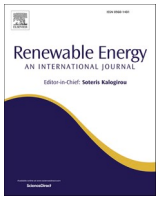



Rubber seed oil biodiesel synthesis via ethanolysis using a blend of four biogenic residues as a sustainable heterogeneous catalyst

Chiazor Faustina Jisieike [a], Eriola Betiku [b,*], Tunde V. Ojumu [c], Lekan M. Latinwo [b]

[a] School of Engineering Technology, Department of Mechanical Engineering, Federal Polytechnic, Oko, Anambra State, Nigeria
[b] Department of Biological Sciences, Florida Agricultural and Mechanical University, Tallahassee, FL, 32307, USA
[c] Department of Chemical Engineering, Cape Peninsula University of Technology, Bellville Campus, Symphony Way, Bellville, Cape Town, 7535, South Africa

ARTICLE INFO

Keywords:
Biodiesel
Taguchi
Transesterification
Rubber seed
Optimization
Heterogeneous catalyst

ABSTRACT

Converting biogenic residues into value-added products is essential to reduce biodiesel production costs and combat environmental pollution. This study developed nanoparticles from ripe plantain peel, fluted pumpkin (*ugu*), cocoa, and kola nut husks (PUCK) blend as a biocatalyst and a renewable alcohol (ethanol) for biodiesel synthesis from rubber seed oil (RSO). The catalytic activity of the biocatalyst was examined through Brunauer-Emmett-Teller-Barret-Joyner-Halenda - BET-BJH, scanning electron microscope-Energy-dispersive X-ray - SEM-EDX, X-ray diffraction - XRD, and Fourier transform infrared spectroscopy - FT-IR analyses. The Taguchi orthogonal array (L9) technique was utilized to model the transesterification process and optimize the independent variables. The optimum RSO ethyl esters (RSOEE) yield of 93.05 ± 0.11 wt% was attained at 1.5 wt% PUCK loading, 60 °C temperature, 40 min reaction time, and a 9:1 ethanol-RSO molar ratio. The biocatalyst reveals significant metallic content, with potassium (K) exhibiting the highest fraction of 47.95 % at 300 °C for 4 h. The biocatalyst demonstrates excellent performance with consistent activity under optimized parametric conditions, sustaining a biodiesel yield of over 85 wt% even past the fifth recycle. The RSOEE characteristics satisfied the biodiesel standard specifications. RSOEE represents an entirely renewable fuel, as all its components, oil, biocatalyst, and ethanol, can be derived from biomass resources.

1. Introduction

Amid climate change challenges and the search for sustainable alternatives to fossil fuels, biodiesel production emerges as a promising technology to improve energy security. Biodiesel is a renewable fuel produced through chemical reactions using vegetable oils, animal fats, lipids from algae, or waste cooking oil with low molecular weight alcohol suitable for use in diesel engines either independently or blended with diesel fuel [1]. It has been shown to have excellent eco-friendly properties, potential for enhancing energy security, compatibility with existing infrastructure, and positive economic impacts [2]. Recently, researchers have thoroughly explored innovative methods to enhance the sustainability of biodiesel production, recognizing economic factors as the most significant threat to its viability. In response to these challenges, the transesterification process has become widely adopted for biodiesel synthesis [3]. However, a critical aspect of ensuring the cost-effectiveness of biodiesel adoption lies in identifying abundantly available biomass feedstock [4]. Consequently, researchers have increased their attention towards employing non-edible oils [5] and algae [6] to address the imbalance between consumer needs and food supplies due to the widespread use of edible oils while mitigating the rising energy needs. Rubber seed oil (RSO) is a promising option among the various feedstock sources due to its abundance and renewable characteristics [7].

Integrating catalysts into the biodiesel production process shows potential for optimizing product efficiencies. This can manifest in various ways, from reducing energy consumption and waste generation to enhancing yield and selectivity [8]. Transitioning from homogeneous acid catalysts to heterogeneous catalysts is essential due to their simpler separation methods, reduced effluent discharge, compatibility with continuous processing, and lowered capital and energy expenses [9]. Moreover, their potential for recycling and reuse can contribute to lowering biodiesel production costs. Several studies have indicated that heterogeneous catalysts offer a superior option to other catalysts, as they facilitate complete methanolysis without generating soap and achieve yields of over 70 % [10]. World's wealth of biomass resources presents opportunities for heterogeneous catalysis, as biogenic residues rich in

* Corresponding author.
E-mail address: eriola.betiku@famu.edu (E. Betiku).

https://doi.org/10.1016/j.renene.2025.123500
Received 23 October 2024; Received in revised form 5 May 2025; Accepted 18 May 2025
Available online 19 May 2025
0960-1481/© 2025 Elsevier Ltd. All rights are reserved, including those for text and data mining, AI training, and similar technologies.

List of abbreviations

BET	Brunauer-Emmett-Teller
BJH	Barret-Joyner-Halenda
EDX	Energy-dispersive X-ray
FT-IR	Fourier transform infrared
PUCK	Plantain peel-ugu-cocoa-kola nut
RSO	Rubber seed oil
RSOEE	Rubber seed oil ethyl esters
SEM	Scanning electron microscope
XRD	X-ray diffraction

necessary components remain largely untapped. Redirecting attention towards utilizing these materials could effectively reduce biodiesel production costs. Recent studies have shown that various biomass materials exhibit high catalytic potential. For instance, banana wastes [11], cocoa pod husk [12], onion peel [13], eggshell [14], plantain peel [15], banana peduncle [16], elephant-ear tree pod husk [17], brassica nigra plant [18], kola nut husk [19], and sandbox shell waste [2] are among those studied.

Combining different biogenic residues can result in synergistic effects, with the resulting catalyst exhibiting enhanced catalytic activity or selectivity compared to individual sources [3]. Mixing the residues allows for the optimization of catalyst properties and enables the utilization of multiple wastes, aligning with the principles that maximize resource efficiency and reduce waste disposal. Also, applying a particular biogenic residue in developing catalysts may be restricted to a certain location due to the non-availability of the waste in a sufficient amount in another location [10]. To address the shortage of catalyst precursors, waste biomaterials readily available are combined to create heterogeneous catalysts. Catalysts sourced from different biogenic residue blends have been successfully utilized in biodiesel production, demonstrating high yields. For instance, Falowo et al. [3] reported a 98.45 wt% biodiesel yield with a catalyst derived from a calcined mixture of kola nut husk, plantain peel, and cocoa husk used to catalyze rubber, honne, and neem oil blend via microwave irradiation. Using calcined plantain peel and cocoa husk, biodiesel obtained from honne seed oil achieved an optimal yield of 98.98 wt% [12]. In another study, cocoa, fluted pumpkin, and kola nut wastes were blended to produce an active alkaline catalyst and applied to the yellow oleander-RSO mixture transesterification with a reported 95.02 wt% biodiesel yield [10].

Selecting a suitable alcohol in biodiesel manufacturing is particularly important because it influences the efficiency, cost-effectiveness, and environmental impact of the process. Various factors, including alcohol pricing, quantity needed, ease of recovery and reuse, fuel tax incentives, and concerns about climate change, collectively impact the selection of appropriate alcohol for biodiesel production [20]. Methanol and ethanol are widely used owing to their low cost. Although glycerol settles slower with ethanol in a biodiesel mixture than methanol because it has a higher molecular weight and viscosity [21], the preference for ethanol over methanol in biodiesel production stems from its renewability, lower toxicity, and reduced environmental impact [22]. Additionally, ethanol can be derived from various renewable sources, including agricultural wastes or biomass [23], making it a more sustainable option. These attributes make ethanol the preferred choice for this study.

Applying process optimization techniques in biodiesel production processes is essential for achieving economic viability and enhanced product quality. The Taguchi factorial design is a statistical method used in experimental design to optimize the performance of systems and processes. Unlike conventional single-variable experimentation, Taguchi's method allows multiple factors and their interactions to be studied simultaneously [24]. Another key feature of the Taguchi method lies in its use of orthogonal arrays in the experimental design. This approach identifies key parameters impacting product quality while minimizing experimental runs [25], thus optimizing time and resource utilization throughout the experimentation process [12]. It has been used in the modeling of transesterification processes [26].

This study addresses the challenge of waste management in agro-based industries and farms by producing an active and efficient base biocatalyst from a blend of four biogenic residues (fluted pumpkin husk, kola nut husk, cocoa husk, and plantain peel) applied in the transesterification of a non-edible oil (RSO) with renewable alcohol (ethanol) to produce biodiesel. Also, the transesterification process was modeled, and pertinent input variables (ethanol/oil ratio (EOR), temperature, reaction time, and catalyst concentration) were optimized using the Taguchi factorial design approach to improve process performance and efficiency. Detailed characterization of the biocatalyst and resultant RSO ethyl esters (RSOEE) provide insights into the potential applications of the novel biodiesel product as a biofuel. This is the first report on synthesizing an alkaline biocatalyst derived from a combination of plantain peel, fluted pumpkin, cocoa, and kola nut husks and its application in the transesterification of RSO. The study aims to contribute to a greener, more sustainable future where waste becomes valuable energy resources.

2. Experimental

2.1. Materials

Jisieike et al. [7] previously documented the characteristics of the RSO utilized in this investigation. The free fatty acid (FFA) content of the RSO was reduced from 22.20 % to 0.56 % under esterification conditions of 16.97 wt% $Fe_2(SO_4)_3$ loading, 44.21:1.00 methanol:RSO, 3.39 h time, and 65 °C temperature. Analytical-grade chemicals and reagents were used for the investigation.

2.2. Catalyst development

The precursors employed in the catalyst development (fluted pumpkin (ugu), kola nut, cocoa husks, and ripe plantain peel) were sourced in Ile-Ife, Nigeria. The waste materials were rinsed separately with distilled water, chopped into little portions, and sun-dried for 2 weeks. Subsequently, they were subjected to oven-drying at 80 °C for 48 h until they achieved a consistent weight. Each waste biomass was combusted in the air individually to generate ash, which was then pulverized into fine particles. The fine particles obtained from each waste were weighed equally, blended, and subjected to calcination using a furnace over 300–1100 °C for 4 h to identify the best calcination temperature [27]. The calcined ash mix, PUCK (plantain-*ugu*-cocoa-kola nut), was sealed in plastic containers and kept in a desiccator.

2.3. PUCK catalyst characterization

The active functional groups of the PUCK catalyst were detected with potassium bromide (KBr) by Fourier infrared transform (FT-IR) spectroscopy using a PerkinElmer Spectrum 100 FTIR spectrophotometer. This analysis was performed using a resolution of 4 cm^{-1} over a range between 4000 and 400 cm^{-1} wavelength, as described earlier [27]. The surface structure and elemental compositions of the PUCK catalyst were analyzed with a scanning electron microscope (SEM) by Auriga Zeiss, Germany, integrated with an energy-dispersive X-ray (EDX) analyzer operated at 10 keV with an Oxford X-Max 20 mm^2. X-ray diffraction (XRD) analysis was performed with a D8 Advance diffractometer manufactured by Bruker AXS, Karlsruhe, Germany, with Cu Kα radiation ($\lambda K\alpha 1 = 1.5406$ Å) fitted with a LynxEye position-sensitive detector to determine the mineral composition of the crystalline materials in the heat-treated ashes. The physisorption properties of the PUCK catalyst were examined using the Micromeritics ASAP 2020 V4.03 equipment (USA), which operates on the principles of gas adsorption and

Table 1
Independent variables for the in the transesterification.

Factor	Unit	Coded factor levels		
		1	2	3
EOR (*A*)	–	6:1	9:1	12:1
PUCK loading (*B*)	wt.%	1.5	2.5	3.5
Temperature (*C*)	°C	45	60	75
Time (*D*)	min	40	55	70

Table 2
Design matrix and RSOEE yields using the Taguchi Method.

Run	Actual factors				RSOEE yield	
	EOR	PUCK loading (wt.%)	Temperature (°C)	Time (min)	Actual (wt.%)	Predicted (wt.%)
1	6:1	3.5	75	70	90.91	90.25
2	6:1	2.5	60	55	88.80	89.22
3	9:1	1.5	60	70	93.87	93.21
4	12:1	2.5	45	70	76.71	76.05
5	9:1	3.5	45	55	85.55	85.97
6	12:1	1.5	75	55	83.90	84.32
7	6:1	1.5	45	40	85.38	85.63
8	9:1	2.5	75	40	86.53	86.78
9	12:1	3.5	60	40	86.84	87.09

desorption using liquid nitrogen at a temperature of 77 K, with the relative pressure range (p/p_o) from 0.01 to 1.0 [27]. The Brunauer-Joyner-Halenda (BJH) technique was used to obtain the pore size distribution and pore volume of the PUCK from the isotherms. The specific surface area of the PUCK was determined using the Brunauer-Emmett-Teller (BET) method. Before the analysis, samples were degassed overnight in an oven at 393 K under vacuum to eliminate moisture.

2.4. Experimental design for the RSOEE synthesis

A Taguchi fractional factorial design with four factors and three levels (Table 1) was utilized to generate different experimental conditions (Table 2). The independent variables selected were PUCK loading (1.5–3.5 wt%), EOR (6:1–12:1), reaction time (40–70 min), and temperature (45–75 °C) with RSOEE yield as the response. Nine experiments were produced (Table 2) using Eq. (1).

$$X = 1 + (Y - 1)^{*}Z \tag{1}$$

where *X*, *Y*, and *Z* represent the number of experiments, the chosen levels, and the number of variables, respectively.

Modeling and regression analysis were conducted using Design Expert version 10.0 software developed by Stat-Ease Inc., USA. The process variables under investigation were optimized by solving the model equation. Each variable impact on the RSOEE yield was measured using Eq. (2).

$$\text{Impact} = \frac{\text{SoS of individual variable}}{\text{Total SoS}} * 100 \tag{2}$$

Where SoS is the sum of squares.

2.5. Biodiesel synthesis by transesterification

The transesterification experiments were conducted by placing a 250-mL round-bottom flask with three necks on a hotplate fitted with a reflux system for cooling. The developed PUCK catalyst was applied, while ethanol was used as the alcohol of choice according to the experimental design. On the completion of the reaction, the reactor contents were transferred into centrifuge tubes, and the centrifuge machine was used to separate the resulting mixture at 8000 rpm for 5 min. Impurities such as unreacted catalyst, ethanol, and residual glycerol in the RSOEE layer were removed by warm water treatment using distilled water at 50 °C. The RSOEE was heated with sodium sulfate at about 100 °C to remove any remaining water in the ester layer. The RSOEE yield was calculated gravimetrically, as given in Eq. (3). The fuel characteristics of the RSOEE were evaluated as described in our previous report [19]. The functional groups in the RSOEE were identified using a Shimadzu 8400S FTIR spectrometer [19].

$$RSOEE\ Yield\ (wt.\%) = \frac{RSOEE\ (g)}{Esterified\ RSO\ used\ (g)} \times 100 \tag{3}$$

3. Results and discussion

3.1. Characterization of the PUCK catalyst

3.1.1. Elemental analysis

The elemental compositions of the PUCK at various temperatures are displayed in Table 3. Notably, the samples contain significant amounts of metallic elements, including K, Ca, Na, and Mg. Although traces of other elements were present, they were in negligible amounts. It is worth noting that the catalytic activity and selectivity of the ash are intricately linked to its chemical composition, with the calcination temperature exerting a significant influence on its properties [19]. Subjecting the ash to elevated temperatures results in a decrease in the oxygen contents during combustion. At 300 °C, K exhibits the highest percent mass fraction compared to the other temperatures examined.

Also, K has been reported to have the highest percent mass fraction among the other metals found in the three biogenic residues used in this study (Table 4). Furthermore, K has been demonstrated to be the primary active ingredient driving catalyst activity in biodiesel synthesis, as highlighted in studies on banana wastes [11], kola nut [19], pawpaw trunk [27], and sandbox [2] residues.

Combining the individual agricultural wastes at a low temperature was identified as an economically viable strategy for sustainable biodiesel synthesis (Table 4). K has been found to have high concentrations in plantain and cocoa waste blend [12] and kola nut, cocoa, and plantain waste blend [3]. The synthesized PUCK catalyst is environmentally safe and non-toxic because it does not contain heavy metals such as mercury, titanium, cadmium, arsenic, and lead [30].

3.1.2. Surface morphology results

The images in Fig. 1(a and b) depict the structure and elemental profile of the PUCK catalyst at 300 °C. Several microporous aggregates

Table 3
PUCK compositions by EDX.

Temperature (°C)	Elements (mass %)											
	O	Mg	Si	P	S	Cl	K	Ca	Fe	Zn	Na	Al
300	42.04	2.96	0.97	1.98	1.22	2.88	47.95	0.00	0.00	0.00	0.00	0.00
500	40.28	3.08	0.90	1.89	1.22	2.26	46.99	3.97	1.85	0.00	0.00	0.00
700	38.75	4.87	1.10	1.62	0.83	2.68	44.41	4.70	1.64	0.65	0.60	0.56
900	38.55	1.98	1.37	2.12	1.21	2.39	46.38	4.70	0.81	1.04	0.42	0.00
1100	35.13	3.88	2.37	1.83	0.00	0.00	39.36	6.45	1.72	0.00	10.14	0.00

Table 4
Compositions of PUCK catalyst and the individual agricultural wastes.

Catalyst	Temperature (°C)	Elements (%)										Ref.
		O	Mg	Si	P	S	Cl	K	Ca	Fe	Al	
PUCK	300	42.04	2.96	0.97	1.98	1.22	2.88	47.95	–	–	–	This work
RPP	500	35.34	3.61	3.87	1.84	0.47	6.27	51.02	–	–	0.29	[28]
CPH	700	36.20	3.00	0.30	0.80	0.70	–	59.20	–	–	–	[29]
KNPH	500	31.07	5.32	0.00	2.31	2.16	4.41	47.14	7.59	–	–	[19]

(RPP) ripe plantain peel, (CPH) cocoa pod husk, (KNPH) kola nut pod husk ash.

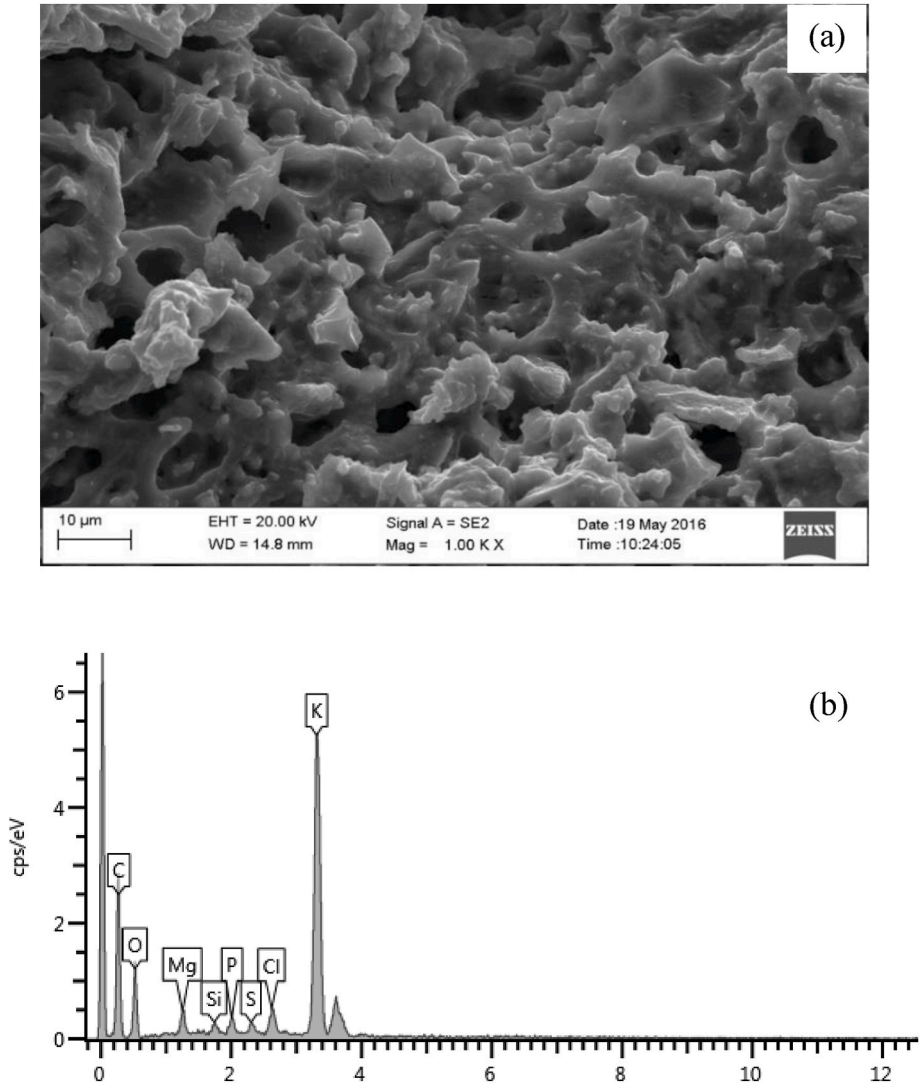

Fig. 1. Micrograph (a) and EDX (b) analyses of PUCK catalyst.

were observed, indicating significant morphological changes from the calcination process.

The SEM image displays clusters of granules with well-defined pores, suggesting an increase in surface area resulting from a reduction in particle size. This characteristic is vital for enhancing the catalytic activity of the PUCK catalyst. The porous structure of the PUCK catalyst could enable it to absorb moisture effectively, an essential feature considering that pretreated or waste oils often contain moisture. Catalysts capable of absorbing moisture support the forward reaction. Thermal treatment of the catalyst through calcination enhances the agglomeration of metallic contents, thereby increasing its reusability and preventing the leaching of K [28]. Similar morphological characteristics have been reported in ashes from various agricultural residues, including kola nut [19], pawpaw trunk [27], sandbox [2] residues, and plantain and cocoa waste blend [12] and kola nut, cocoa, and plantain waste blend [3].

3.1.3. Diffractogram pattern and infrared spectrum of the PUCK catalyst

Fig. 2a represents the x-ray diffraction profile of the PUCK catalyst. The peaks in the figure correspond to distinct crystalline components, including KCl, $K_2Ca(CO_3)_2$, and $K_2CO_3.5H_2O$. The diffractogram reveals that K exists predominantly as carbonates and chlorides, confirming its high basicity as indicated in Table 3. These findings align with similar crystalline phases observed in various calcined biogenic residues in previous studies on banana wastes [11], sugarcane bagasse [31], and plantain wastes [15].

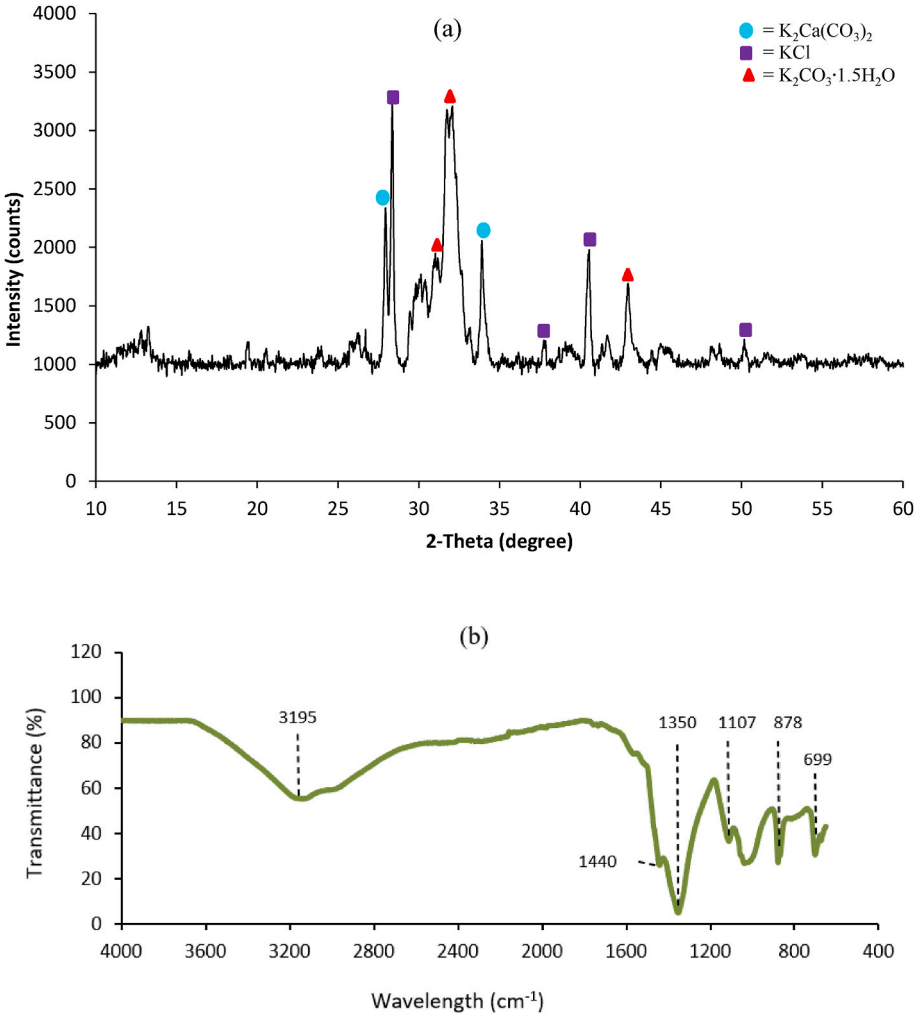

Fig. 2. Diffractogram pattern (a) and infrared spectrum (b) of the PUCK.

Fig. 2b describes the FT-IR spectrum, illustrating the vibration frequencies of various functional groups in the PUCK catalyst. A band at 3195 cm^{-1} suggests the existence of a weakly bonded O-H functional group from a water molecule attached to the surface, as observed in catalysts derived from kola nut [19], pawpaw trunk [27], and sandbox shell [2]. The stretching vibrations of the C–O bond detected at 1350 cm^{-1} signifies the existence of carbonate (CO_3), a characteristic feature associated with K_2CO_3 as corroborated by the XRD spectrum [2].

The appearance of bands corresponding to basic carbonates within the 1500 - 1300 cm^{-1} range may be ascribed to the entrapment of CO_2 on the basic sites of K_2O. Similar results have been documented in previous studies on pawpaw trunks [27] and sandbox shells [2]. Peaks at 1107, 1020, 878, and 699 cm^{-1} are linked to the symmetric stretching vibrations of Si-O-Si and Si-OH bonds [11]. The strong peak observed at 1440 cm^{-1} indicates C-H bending vibrations of the alkane groups, while the peaks in the 1400-1200 cm^{-1} range confirm the bending vibrations of CH_2 and CH_3 aliphatic groups. Additionally, a strong peak at 878 cm^{-1} suggests symmetric nitrate ion stretching vibrations [19].

3.1.4. *Surface characteristics of the PUCK catalyst*

BET-BJH analysis was conducted to characterize further the novel biocatalyst synthesized, viz. surface area, pore volume, pore size distribution, and pore diameter, which are critical factors affecting the catalytic performance of catalysts. The surface area of the PUCK catalyst at 77.3 K measures 6.2389 m^2/g alongside a pore volume of 0.040321 cm^3/g and an average pore size of 25.85 nm. The PUCK catalyst exhibits

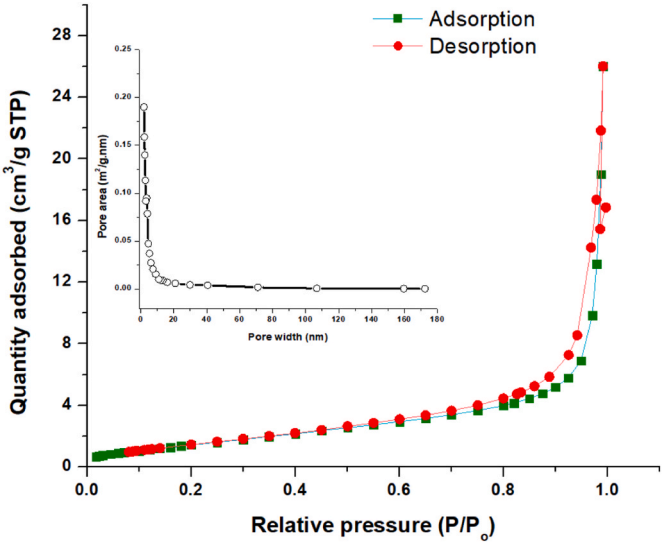

Fig. 3. Physisorption isotherms and pore-size distribution of PUCK.

a pore diameter comparable to other biogenic residue-based catalysts [2]. The physisorption isotherms (Fig. 3) of the PUCK catalyst bear a resemblance to type *IV* with adsorption hysteresis *H3* that moved at a

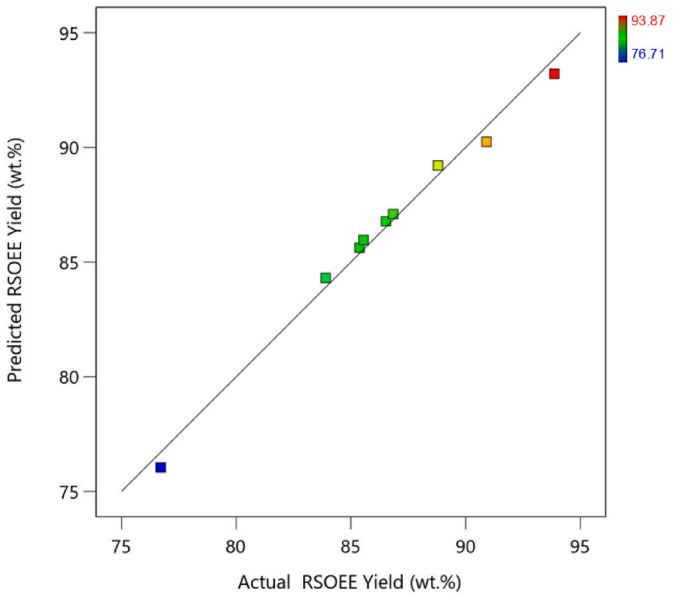

Fig. 4. Plot showing the actual and predicted values of RSOEE yield.

relative pressure greater than 0.8, indicating a mesoporous material [19].

These characteristics suggest active sites with an appropriate pore configuration corresponding to their catalytic activity. Moreover, Fig. 3 further confirms the mesoporous structure of the PUCK catalyst, characterized by a pore diameter between 2 and 50 nm [15]. On the textural properties of individual biogenic residue ashes, Etim et al. [28] analyzed ripe plantain peel ash heated at 700 °C for 4 h, reporting surface area, pore volume, and pore diameter values of 18.8000 m^2/g, 0.032122 cm^3/g, and 6.8300 nm, respectively. Similarly, Betiku et al. [19] investigated kola nut waste (heated at 500 °C for 4 h), revealing surface area, pore volume, and pore diameter measurements of 5.2199 m^2/g, 0.012200 m^3/g, and 9.3174 nm, respectively. Furthermore, Betiku et al. [2] examined sandbox waste heated at 500 °C for 4 h, yielding surface area, pore volume, and pore diameter values of 6.1125 m^2/g, 0.024444 m^3/g, and 18.0100 nm, respectively. These findings collectively suggest that blending the catalysts demonstrates improved surface area and pore volume in contrast to the individual biogenic residues, thus suggesting a more favorable catalytic activity.

3.2. Taguchi modeling for the transesterification process

The RSOEE yield varied between 76.71 and 93.87 wt%, with run 3 having the highest yield, as presented in Table 2. Eq. (4) describes the response's relationship with the independent variables in coded factors.

$$RSOEE\ yield\ (wt.\%) = 86.50 + 1.86A[1] + 2.15A[2] + 1.22B[1] - 2.49B[2] - 3.95C[1] + 3.34C[2] \quad (4)$$

where A [1] and A [2] represent the EOR, B [1] and B [2] indicate the PUCK loading (wt.%), and C [1] and C [2] correspond to the reaction temperature (°C) at the first and second levels, respectively.

The model equation was generated by removing statistically insignificant factors. The impact of reaction time on the RSOEE yield was minimal, so it was excluded from the model equation. Fig. 4 depicts the plot of actual data alongside the predictions generated by the model. Table 5 shows the coefficients for the model and independent factors at the 95 % confidence level. The model is statistically significant based on the F-value (29.89) and the p-value (0.0327). The ANOVA results further revealed that temperature and EOR impacted RSOEE yield significantly (Table 5).

It is evident from Fig. 5 that temperature (44.27 %) had the highest effect on the RSOEE yield. This was followed by the EOR (39.51 %) and PUCK loading (15.11 %). The impact of the reaction time is negligible (1.10 %), primarily because 40 min proved sufficient for the RSO transesterification.

An R^2 of 0.9890 suggests that the actual data fits the model satisfactorily since the value is close to 1.0 [27]. The value suggests that the data linearly aligns with the trendline. The predicted R^2 value of 0.7767 is reasonably consistent with the adjusted R^2 value of 0.9559, having a variance of less than 0.2. The standard deviation was determined to be 1.01 with a coefficient of variation (CV) of 1.16 %, suggesting the validity and feasibility of the model. The low values indicate a high degree of reliability of the model [2]. The average response yielded a value of 86.50. Adequate precision was assessed through the overall

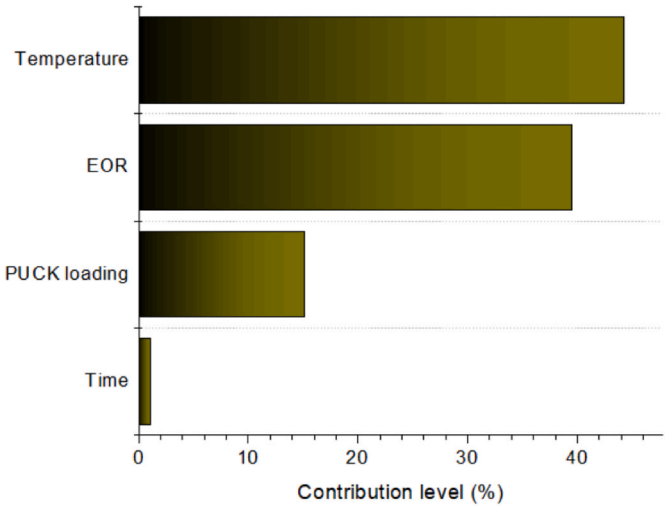

Fig. 5. The impact level of process variables on RSOEE yield.

Table 5
Model statistics estimated

Source of Variance	SS	Df	Mean square	F-value	p-value	Accuracy test	
						Parameter	Value
Model	181.90	6	30.32	29.89	0.0327	R^2	0.9890
A - EOR	72.68	2	36.34	35.83	0.0271	Adjusted R^2	0.9559
B - PUCK loading	27.80	2	13.90	13.71	0.0680	Predicted R^2	0.7767
C - Temperature	81.42	2	40.71	40.14	0.0243	Mean of response	86.5000
Residual	2.03	2	1.01			Adequate precision	19.3210
Total	183.93	8				Standard deviation	1.0100
						CV (%)	1.16
						PRESS	41.0700

SS – sum of squares, Df – degree of freedom, CV – coefficient of variance, PRESS – predicted residual error sum of squares

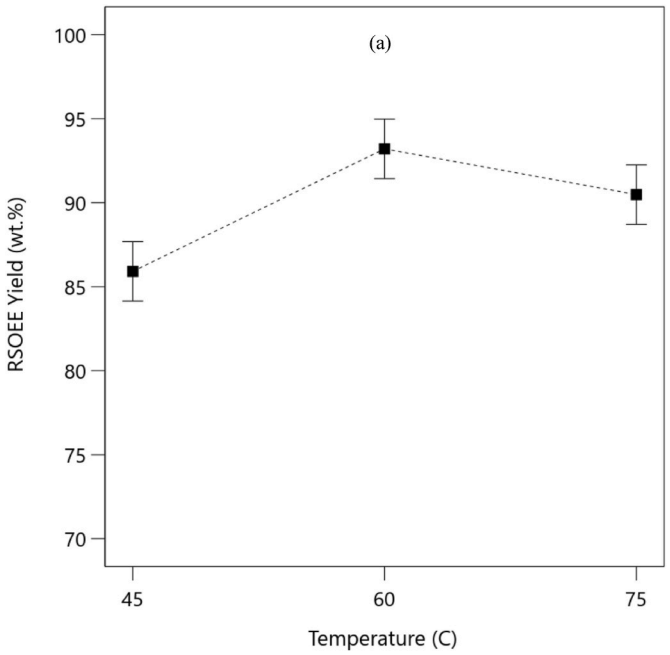

Fig. 6a. Effect of temperature on RSOEE yield.

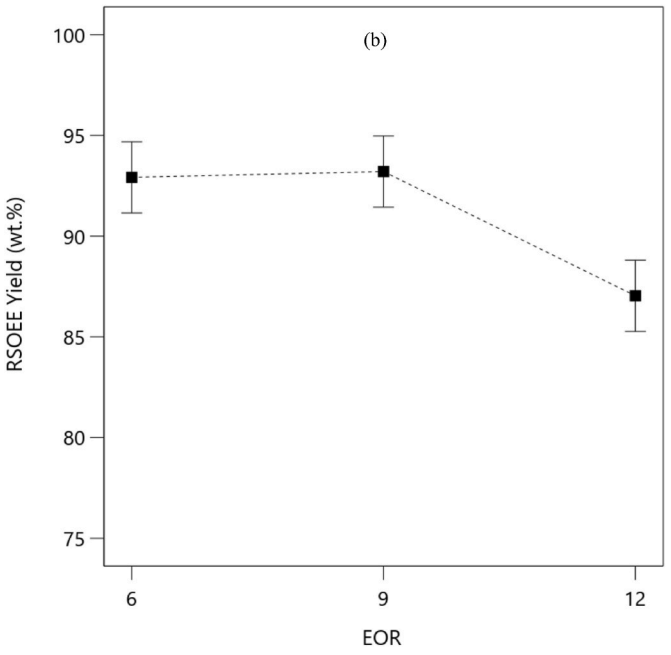

Fig. 6b. Effect of EOR on RSOEE yield.

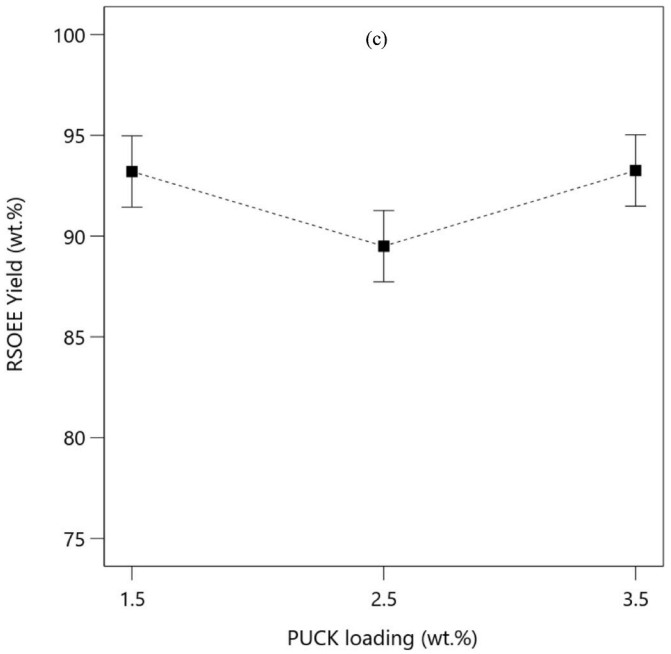

Fig. 6c. Effect of PUCK loading on RSOEE yield.

signal-to-noise ratio (SNR), calculated to be 19.3210, indicating a robust signal suitable for optimization. A high SNR indicates a stronger, clearer signal than the noise, resulting in more accurate and reliable results. The predicted residual sum of squares was calculated for every data point and determined to be 41.07, suggesting that each point fits well into the design [27].

3.3. Impact of process variables on RSOEE yield

The results of this study demonstrate that the reaction temperature, EOR, and PUCK loading impacted the RSOEE yield. Consequently, their effects on the RSOEE yield were investigated. Time exhibited a non-significant influence on the RSOEE yield and was thus excluded from further consideration.

3.3.1. Effect of temperature on RSOEE yield

Fig. 6a shows the temperature effect on the RSOEE yield when the study was conducted using an EOR of 9:1, PUCK loading of 1.5 wt%, and time of 40 min.

The figure illustrates that increasing the temperature enhanced the RSOEE yield significantly. The highest RSOEE yield of 93.87 wt% was attained at a temperature of 60 °C, an EOR of 9:1, a PUCK loading of 1.5 wt%, and a time of 40 min. The influence of reaction temperature was more significant at low PUCK loading but decreased as the loading increased. Changing the temperature from 45 to 60 °C enhances the RSOEE yield by accelerating the reaction rate. This could result from the increased attraction of the carbonyl group in FFA to the nucleophilic alcohol at elevated temperatures [32]. This intensifies activation to its peak, prompting the reaction to progress in the forward direction, thereby maximizing biodiesel yield. However, increasing the temperature to 75 °C reduces the RSOEE yield. This could be due to the conversion of ethanol to vapor as it tends towards its boiling point (78.37 °C), thereby decreasing the volume of the reaction mixture and the biodiesel yield. The reduced RSOEE yield at elevated temperatures could also be linked to the decline in alcohol polarity at high temperatures [27]. Also, biodiesel yield decreases because of the saponification of triglycerides, which accelerates at high temperatures [33]. A report on reduced biodiesel yield due to saponification at high temperatures was on the transesterification of fish oil and heterogeneous catalyst produced from eggshell and copper oxide when the temperature was increased beyond 80 °C with ethanol as the alcohol [34]. Using ethanol for transesterification produces more saponification than methanol due to more hydroxyl ions [35].

3.3.2. Effect of EOR on RSOEE yield

The stoichiometry of the transesterification reaction imposes 1 mol of oil and 3 mol of alcohol for ester formation. Nevertheless, a higher mole of alcohol is needed to drive the reaction toward completion, but an excess supply could result in dilution, which could lower the biodiesel yield [28]. The EOR was investigated across three levels (6:1, 9:1, and 12:1) to examine its influence on RSOEE yield while keeping the temperature at 60 °C, PUCK loading at 1.5 wt%, and time at 40 min. As

presented in Fig. 6b, the RSOEE yield slightly increased from 6:1 to 9:1. However, increasing the molar ratio to 12:1 significantly reduced the yield. At high molar ratios, alcohol has been noted to potentially impede glycerol separation by enhancing the solubility of glycerol in alcohol, thereby resulting in a reduction in yield [36]. The reduction in yield could also be linked to a decrease in oil concentration relative to ethanol concentration, which poses a challenge in glycerol separation [28]. The decrease in oil conversion at the 12:1 M ratio could also be linked to reverse transesterification at high alcohol ratios [2].

3.3.3. Effect of PUCK loading on RSOEE yield

The effect of PUCK loading was investigated by varying it at three levels (1.5, 2.5, and 3.5 wt%) while keeping the EOR of 9:1, temperature of 60 °C, and time of 40 min (Fig. 6c). RSOEE yield of 93.87 wt% was obtained using the PUCK loading of 1.5 and 3.5 wt%. However, the yield was reduced when the PUCK loading was 2.5 wt%.

The reduction in RSOEE yield with an increase in the catalyst may be attributed to the higher mass transfer resistance of the reaction mixture at elevated catalyst concentrations [37]. Also, the decrease in the RSOEE yield may be due to soap formation via saponification rather than biodiesel formation via transesterification [38]. The later increase in the yield when the catalyst loading was increased may be due to the reverse reaction. This type of observation has been reported in the literature on other input variables such as reaction time [39], alcohol-to-oil ratio [40], and reaction temperature [38]. Therefore, low catalyst loading can produce the best yield because of the availability of basic sites in the developed catalyst. This benefits the overall process since only a small amount of the PUCK catalyst is needed for maximum biodiesel yield, potentially lowering the production costs.

3.4. Model validation via experimentation and optimization

The process variables should be optimized to produce biodiesel at an economically viable cost. The study determined that the best conditions for converting RSO into RSOEE were an EOR of 9:1, a PUCK loading of 1.5 wt%, a temperature of 60 °C, and a reaction time of 40 min. A maximum RSOEE yield of 93.21 % was predicted with a desirability of 0.9610. Confirmatory experiments conducted in triplicate confirmed the optimal conditions, yielding an average of 93.05 ± 0.11 wt%. The observed similarity between experimental and predicted yields suggests that the regression model is effective and could be used to estimate the optimum conditions for RSOEE production using a PUCK catalyst. The RSO biodiesel yield observed when methanol was used was 97.14 wt% with MOR of 6:1, temperature of 65 °C, time of 75 min, and catalyst (from kola nut waste) loading of 3.5 wt% [41]. In another study on RSO, an 81.55 % yield was reported with MOR of 6:1, temperature of 60 °C, time of 90 min, and catalyst (NaOH) loading of 1 % [42]. Also, a 98.10 wt% RSO biodiesel yield was observed using conditions of MOR 9:1, catalyst (Fe/C) loading 4.5 wt%, temperature 60 °C, and agitation speed of 1250 rpm [43]. The higher biodiesel yields observed in earlier reports [41,43] is attributable to methanol, which is more reactive than ethanol employed in the current study [44]. A biodiesel yield of 86.69 % was reported when palm kernel oil and ethanol were used under optimal conditions of EOR of 12:1, temperature of 65 °C, time of 40 min, and catalyst (from periwinkle shell, melon seed husk, and locust bean pod husk) loading of 37 wt% [45]. Higher biodiesel yields (99.5 wt% for banana peel-based catalyst and 99.3 wt% for cocoa waste-based catalyst) were reported for the transesterification of palm kernel oil with methanol under optimal conditions MOR of 0.8 v/v, catalyst weight of 4 wt%, time of 65 min, and temperature of 65 °C [46].

3.5. PUCK catalyst stability test

Employing biomass-based catalysts could reduce biodiesel production costs through reuse and recycling while minimally impacting the overall biodiesel yield. The potential reusability of the PUCK catalyst was assessed under conditions established in this work without any further treatment. The PUCK catalyst recovered from the first transesterification cycle was isolated from the resulting products through centrifugation. The recovered catalyst was utilized for subsequent cycles of biodiesel synthesis. The performance of the PUCK catalyst was studied across six cycles, as represented in Fig. 7. The slight decrease the RSOEE yield in each reaction cycle could be caused by glycerol trapping on its active surface [2]. Another possible reason could be the blocking of active sites caused by the buildup of organic materials on the catalyst surface, along with the leaching of active metals into the reaction medium.

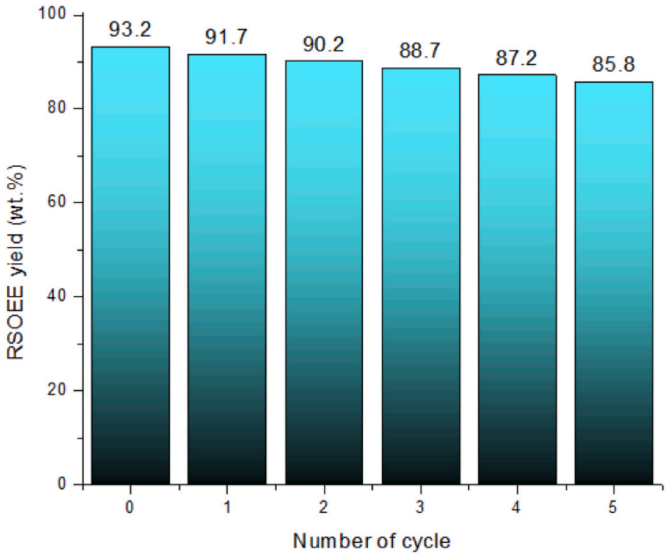

Fig. 7. Reusability test for calcined PUCK catalyst.

The reusability result suggests good stability and recyclability of the PUCK catalyst for biodiesel synthesis. It has been reported that blending biogenic residues for catalyst synthesis offers a promising solution to the high production costs of biodiesel due to its appreciable reuse potential and the combination of metallic components inherent in the individual waste biomass. Olatundun et al. [12] investigated the reusability potential of a cocoa-plantain waste blend on honne oil biodiesel synthesis and, after three transesterification cycles, reported a slight reduction in catalytic activity. Falowo et al. [3] also conducted a reusability study on the biocatalyst derived from a plantain, cocoa, and kola nut waste blend. They applied this catalyst to the transesterification of a mixture of honne oil, RSO, and neem oil, achieving an 89.46 wt% yield by the 4th cycle.

3.6. Cost evaluation of the PUCK catalyst

The price of the catalyst employed significantly impacts biodiesel production costs. Assessing costs at various stages and in different combinations determines the feasibility of using such low-cost catalysts commercially. The total cost of developing catalysts is frequently tied to factors such as raw material availability, preparation techniques, activation methods, and potential for reuse [50]. The production cost for 1 kg of catalyst prepared under optimal conditions using the method earlier described by Dhawane et al. [50] and Odude et al. [46] is as follows.

1. Cost of materials (COM) = $0.00. The raw materials used are agricultural wastes readily abundant in nature.
2. Cost of washing (COW) = $0.50. The wastes were washed with distilled water obtained from the laboratory.
3. Cost of drying (COD) = $0.00. The wastes were sundried.
4. Cost of milling (MC) = $0.00. The manual process was used for size reduction.

Table 6
Properties of RSOEE produced from this study.

Parameters	This study	Sugebo et al. [42]	Onoji et al. [30]	Saravanan et al. [49]	Dhawane et al. [50]	Khan [51]	Betiku and Oladipo [41]	ASTM D6751	EN 14214
Moisture content (%)	0.006	0.91	–	–	–	–	0.002	<0.050	<0.050
Kinematic viscosity (mm^2/s) at 40°C	5.16 ± 0.12	2.81	4.32	3.62	5.54	3.90	4.98	1.90–6.00	3.50–5.00
Density (kg/m^3) at 25 °C	886.5 ± 1.1	860.0	876.0	872.0	870.0	892.0	887.0	–	860–900
Acid value (mg KOH/g oil)	0.33	0.22	0.56	0.96	0.1	0.07	0.224	0.50 max	0.50 max
Higher heating value (MJ/kg)	40.16	43.87	40.67	–	45.17	37.21	40.32	–	–
Cetane number	52.85	–	57	62	53	52	59.54	47 min	51 min
Cloud point (°C)	+8.0	–	+4.8	+7.0	−7.0	3.0	–	−3.0 – 12.0	–
Pour point (°C)	−1	–	−8	−7	−22	−5	–	−15 - 10	–
Flash point (°C)	180	–	158	162	180	175	–	130 min	101 min

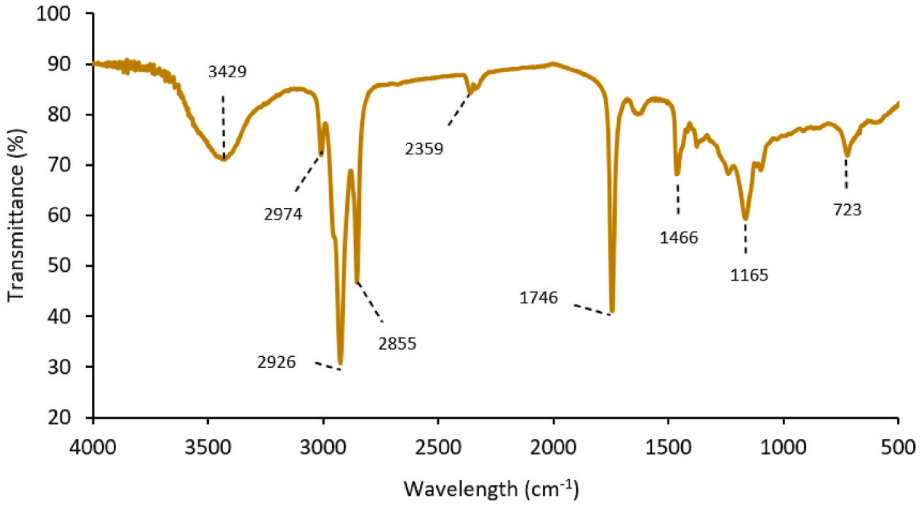

Fig. 8. IR spectrum of RSOEE.

5. Cost of calcination (CC) = hour x unit x cost per unit = 4 × 1 × $0.45 = $1.80
6. Net cost = COM + COW + COD + MC + CC = $2.30.

From this study, the overall cost of producing 1 kg of PUCK catalyst is $2.30. The economic sustainability of the PUCK catalyst lies in its low manufacturing costs and availability of raw materials. Adopting the PUCK catalyst could reduce biodiesel production costs due to its affordability and excellent reusability. Currently, 1 kg of KOH is sold between $110 and $150.

3.7. Physicochemical characterization of RSOEE

The fuel properties of RSOEE synthesized with the PUCK catalyst are displayed in Table 6. The acid value, measured at 0.33 mg KOH/g, indicates that the RSOEE can be safely used in engines without corroding metal components. The cetane number of 52.85 signifies that the RSOEE has high ignition quality. High cetane numbers suggest good combustion properties, making the RSOEE suitable for engine use [47]. The RSOEE exhibits a higher heat value content of 40.16 MJ/kg, indicating enough energy capacity in the combustion products [41] and attributable to the additional carbon atom from the ethanol molecule, demonstrating the energy efficiency of the fuel [41]. The kinematic viscosity measured at 40 °C was 5.16 mm^2/s, which is within the prescribed specifications and consistent with reported values for biodiesel produced from RSO [41]. Fuel with high viscosity can lead to engine deposits, decreasing the atomization necessary for ignition [47]. Therefore, fuels with low viscosity are preferred. The high flash point of 180 °C of the RSOEE confirms its safe storage and transport at room temperature. With pour and cloud points of −1 °C and 8 °C, respectively, the fuel demonstrates suitability for use in cold climates [48].

3.8. IR spectrum of RSOEE

Fig. 8 illustrates the FT-IR spectrum for the RSOEE produced from this study. The spectral band at 3429 cm^{-1} is linked to the –C = O bond [19]. The peaks at 2974-2855 cm^{-1} suggest symmetric and asymmetric stretching and vibration of C–H in the methyl group [11].

The peak at 1746 cm^{-1} is linked to the stretching of the carbonyl group (–C=O), confirming that the resulting product is an ester [19,52]. The asymmetric and symmetric CH_3 deformations were detected at 1466 cm^{-1} and 1377 cm^{-1}, respectively [11]. The region of 1240-1165 cm^{-1} represents the symmetric stretching vibration of the (C–O–C) group. Esters are typically identified by a strong absorption around 1740 cm^{-1} as a result of C=O stretching frequency, and a significant absorption near 1240 cm^{-1} is linked to C-O stretching [19,52]. The alkyl chain vibration is found at 723 cm^{-1}. The results are consistent with previous studies on RSO fatty acid esters [19,52].

4. Conclusions

This study synthesized biodiesel using biomass-derived materials, including RSO, ethanol, and a heterogeneous catalyst (PUCK catalyst) produced from ripe plantain peel, kola nut pod, cocoa pod, and fluted

pumpkin pod husks. The results revealed that temperature and EOR are the most significant parameters influencing the RSOEE yield. At optimal conditions of EOR of 9:1, PUCK loading of 1.5 wt%, temperature at 60 °C, and time of 40 min, a maximum RSOEE yield of 93.05 ± 0.11 wt% was achieved. The developed PUCK catalyst contains significant metallic elements, with K (47.95 %) as the dominant element. The catalytic activity of the PUCK catalyst is primarily driven by its high K content. The surface morphology reveals aggregates with a mesoporous structure with a substantial surface area of 6.2389 m^2/g. The reusability test confirmed the efficiency of the developed PUCK catalyst, and it was reusable up to five times. The properties of the RSOEE met the standard specifications set for biodiesel products. Thus, this study demonstrates that utilizing agricultural wastes for biodiesel production aligns with sustainability principles, effectively addressing environmental and waste management problems.

CRediT authorship contribution statement

Chiazor Faustina Jisieike: Writing – original draft, Methodology, Investigation. **Eriola Betiku:** Writing – review & editing, Supervision, Methodology, Conceptualization. **Tunde V. Ojumu:** Resources, Methodology. **Lekan M. Latinwo:** Resources, Funding acquisition.

Declaration of competing interest

The authors declare that they have no known competing financial interests or personal relationships that could have appeared to influence the work reported in this paper.

Acknowledgments

Special thanks to the Obafemi Awolowo University and Florida A&M University for creating the space to conduct this research.

References

[1] E. Betiku, A. Osunleke, V. Odude, A. Bamimore, B. Oladipo, A. Okeleye, N. Ishola, Performance evaluation of adaptive neuro-fuzzy inference system, artificial neural network and response surface methodology in modeling biodiesel synthesis from palm kernel oil by transesterification, Biofuels 12 (2021) 339–354.
[2] E. Betiku, J.C. Oraegbunam, O.A. Falowo, T.V. Ojumu, L.M. Latinwo, Sustainable microwave-supported biodiesel production using sandbox oil and its waste shell as a nanoparticle green alkali heterogeneous catalyst, Process Biochem. 142 (2024) 1–12.
[3] O.A. Falowo, T.V. Ojumu, O. Pereao, E. Betiku, Sustainable biodiesel synthesis from honne-rubber-neem oil blend with a novel mesoporous base catalyst synthesized from a mixture of three agrowastes, Catalysts 10 (2020) 190.
[4] A.O. Etim, P. Musonge, A.C. Eloka-Eboka, Effectiveness of biogenic waste-derived heterogeneous catalysts and feedstock hybridization techniques in biodiesel production, Biofuel Bioprod. Biorefining 14 (2020) 620–649.
[5] K. Saikia, A. Das, A.H. Sema, S. Basumatary, N.S. Moyon, T. Mathimani, S. L. Rokhum, Response surface optimization, kinetics, thermodynamics, and life cycle cost analysis of biodiesel production from *Jatropha curcas* oil using biomass-based functional activated carbon catalyst, Renew. Energy 229 (2024) 120743.
[6] W. Senusi, M.I. Ahmad, H.A. Khalil, M.A. Shakir, F. Binhweel, E. Shalfoh, S. Alsaadi, Comparative assessment for biodiesel production from low-cost feedstocks of third oil generation, Renew. Energy (2024) 121369.
[7] C.F. Jisieike, N.B. Ishola, L.M. Latinwo, E. Betiku, Crude rubber seed oil esterification using a solid catalyst: optimization by hybrid adaptive neuro-fuzzy inference system and response surface methodology, Energy 263 (2023) 125734.
[8] Y. Zhang, L. Duan, H. Esmaeili, A review on biodiesel production using various heterogeneous nanocatalysts: operation mechanisms and performances, Biomass Bioenergy 158 (2022) 106356.
[9] D.T. Oyekunle, M. Barasa, E.A. Gendy, S.K. Tiong, Heterogeneous catalytic transesterification for biodiesel production: feedstock properties, catalysts and process parameters, Process Saf. Environ. Prot. 177 (2023) 844–867.
[10] O.A. Falowo, E. Betiku, A novel heterogeneous catalyst synthesis from agrowastes mixture and application in transesterification of yellow oleander-rubber oil: optimization by taguchi approach, Fuel 312 (2022) 122999.
[11] S. Brahma, B. Basumatary, S.F. Basumatary, B. Das, S. Brahma, S.L. Rokhum, S. Basumatary, Biodiesel production from quinary oil mixture using highly efficient *Musa chinensis* based heterogeneous catalyst, Fuel 336 (2023) 127150.
[12] E.A. Olatundun, O.O. Borokini, E. Betiku, Cocoa pod husk-plantain peel blend as a novel green heterogeneous catalyst for renewable and sustainable honne oil biodiesel synthesis: a case of biowastes-to-wealth, Renew. Energy 166 (2020) 163–175.
[13] M. Hlaibi, N. Kamil, Highly efficient sustainable heterogeneous catalyst derived from onion peels (*Allium sepa* L.) for the ecological biodiesel production using non-edible feedstock, Energy Convers. Manag. 315 (2024) 118801.
[14] D.K. Jana, S. Bhattacharjee, S. Roy, P. Dostál, B. Bej, The optimization of biodiesel production from waste cooking oil catalyzed by ostrich-eggshell derived CaO through various machine learning approaches, Cleaner Energy Systems 3 (2022) 100033.
[15] O.A. Falowo, B. Oladipo, A.E. Taiwo, A.T. Olaiya, O.O. Oyekola, E. Betiku, Green heterogeneous base catalyst from ripe and unripe plantain peels mixture for the transesterification of waste cooking oil, Chem. Eng. J. Adv. 10 (2022) 100293.
[16] M. Balajii, S. Niju, Banana peduncle–A green and renewable heterogeneous base catalyst for biodiesel production from *Ceiba pentandra* oil, Renew. Energy 146 (2020) 2255–2269.
[17] O.A. Falowo, M.I. Oloko-Oba, E. Betiku, Biodiesel production intensification via microwave irradiation-assisted transesterification of oil blend using nanoparticles from elephant-ear tree pod husk as a base heterogeneous catalyst, Chem. Eng. Process. Process Intensif. 140 (2019) 157–170.
[18] B. Nath, B. Das, P. Kalita, S. Basumatary, Waste to value addition: utilization of waste *Brassica nigra* plant derived novel green heterogeneous base catalyst for effective synthesis of biodiesel, J. Clean. Prod. 239 (2019) 118112.
[19] E. Betiku, A.A. Okeleye, N.B. Ishola, A.S. Osunleke, T.V. Ojumu, Development of a novel mesoporous biocatalyst derived from kola nut pod husk for conversion of kariya seed oil to methyl esters: a case of synthesis, modeling and optimization studies, Catal. Lett. 149 (2019) 1772–1787.
[20] G.M. Mathew, D. Raina, V. Narisetty, V. Kumar, S. Saran, A. Pugazhendi, R. Sindhu, A. Pandey, P. Binod, Recent advances in biodiesel production: challenges and solutions, Sci. Total Environ. 794 (2021) 148751.
[21] I.A. Musa, The effects of alcohol to oil molar ratios and the type of alcohol on biodiesel production using transesterification process, Egypt. J. Petrol. 25 (2016) 21–31.
[22] P. Verma, M. Sharma, G. Dwivedi, Impact of alcohol on biodiesel production and properties, Renew. Sustain. Energy Rev. 56 (2016) 319–333.
[23] V. Narisetty, S. Maitra, A. Tarafdar, M.P. Alphy, A.N. Kumar, A. Madhavan, R. Sirohi, M.K. Awasthi, R. Sindhu, S. Varjani, Waste-derived fuels and renewable chemicals for bioeconomy promotion: a sustainable approach, BioEnergy Research 16 (2023) 16–32.
[24] V. Ayhan, Ç. Çangal, İ. Cesur, A. Çoban, G. Ergen, Y. Çay, A. Kolip, İ. Özsert, Optimization of the factors affecting performance and emissions in a diesel engine using biodiesel and EGR with Taguchi method, Fuel 261 (2020) 116371.
[25] C. Aseibichin, W.C. Ulakpa, I. Omenogor, E. Doyah, A.A. Olaseinde, O. C. Anakpoha, M. Keke, S. Karuppannan, Modeling and optimization of transesterification of jatropha oil to fatty acid methyl ester: application of response surface methodology (CCD) and Taguchi orthogonal method, RSC Adv. 14 (2024) 11784–11796.
[26] W.U. Rahman, A.M. Khan, A.H. Anwer, U. Hasan, B. Karmakar, G. Halder, Parametric optimization of calcined and Zn-doped waste egg-shell catalyzed biodiesel synthesis from *Hevea brasiliensis* oil, Energy Nexus 6 (2022) 100073.
[27] O.A. Fadara, O.A. Falowo, T.V. Ojumu, E. Betiku, Process optimization of microwave irradiation-aided transesterification of kariya seed oil by Taguchi orthogonal array: pawpaw trunk as a novel biocatalyst, Biofuel Bioprod. Biorefining 15 (2021) 1006–1020.
[28] A.O. Etim, E. Betiku, S.O. Ajala, P.J. Olaniyi, T.V. Ojumu, Potential of ripe plantain fruit peels as an ecofriendly catalyst for biodiesel synthesis: optimization by artificial neural network integrated with genetic algorithm, Sustainability 10 (2018) 707.
[29] E. Betiku, A.O. Etim, O. Pereao, T.V. Ojumu, Two-step conversion of neem (*Azadirachta indica*) seed oil into fatty methyl esters using a heterogeneous biomass-based catalyst: an example of cocoa pod husk, Energy Fuels 31 (2017) 6182–6193.
[30] S.E. Onoji, S.E. Iyuke, A.I. Igbafe, M.O. Daramola, Transesterification of rubber seed oil to biodiesel over a calcined waste rubber seed shell catalyst: modeling and optimization of process variables, Energy Fuels 31 (2017) 6109–6119.
[31] B. Basumatary, B. Das, B. Nath, S. Basumatary, Synthesis and characterization of heterogeneous catalyst from sugarcane bagasse: production of jatropha seed oil methyl esters, Current Research in Green and Sustainable Chemistry (2021) 100082.
[32] S. Valizadeh, B. Valizadeh, Y. Khani, J. Jae, C.H. Ko, Y.-K. Park, Production of biodiesel via esterification of coffee waste-derived bio-oil using sulfonated catalysts, Bioresour. Technol. (2024) 130908.
[33] M.E. Günay, L. Türker, N.A. Tapan, Significant parameters and technological advancements in biodiesel production systems, Fuel 250 (2019) 27–41.
[34] V. Sharma, A.K. Hossain, G. Griffiths, G. Duraisamy, J.J. Thomas, Investigation on yield, fuel properties, ageing and low temperature flow of fish oil esters, Energy Convers. Manag. X 14 (2022) 100217.
[35] V.C. Eze, A.P. Harvey, A.N. Phan, Determination of the kinetics of biodiesel saponification in alcoholic hydroxide solutions, Fuel 140 (2015) 724–730.
[36] Y.S. Erchamo, T.T. Mamo, G.A. Workneh, Y.S. Mekonnen, Improved biodiesel production from waste cooking oil with mixed methanol–ethanol using enhanced eggshell-derived CaO nano-catalyst, Sci. Rep. 11 (2021) 1–12.
[37] Z. Yuan, J. Zhu, J. Lu, Y. Li, J. Ding, Preparation of biodiesel by transesterification of Castor oil catalyzed by flaky halloysite supported ZnO/SnO_2 heterojunction photocatalyst, Renew. Energy 227 (2024) 120516.

[38] H. Esmaeili, G. Yeganeh, F. Esmaeilzadeh, Optimization of biodiesel production from *Moringa oleifera* seeds oil in the presence of nano-MgO using Taguchi method, Int. Nano Lett. 9 (2019) 257–263.
[39] S.L. Gadhave, S.S. Ragit, Process optimization of tung oil methyl ester (*Vernicia fordii*) using the Taguchi approach, and its fuel characterization, Biofuels 11 (2020) 49–55.
[40] A.D. Halwe, S.J. Deshmukh, N.J. Kanu, E. Gupta, R.B. Tale, Optimization of the novel hydrodynamic cavitation based waste cooking oil biodiesel production process parameters using integrated L9 Taguchi and RSM approach, Mater. Today Proc. 47 (2021) 5934–5941.
[41] B. Oladipo, E. Betiku, Optimization and kinetic studies on conversion of rubber seed (*Hevea brasiliensis*) oil to methyl esters over a green biowaste catalyst, J. Environ. Manag. 268 (2020) 110705.
[42] B. Sugebo, Z. Demrew, S. Feleke, M. Biazen, Evaluation and characterization of rubber seed oil for biodiesel production, Biomass Conversion and Biorefinery (2021) 1–11.
[43] S.H. Dhawane, A.P. Bora, T. Kumar, G. Halder, Parametric optimization of biodiesel synthesis from rubber seed oil using iron doped carbon catalyst by Taguchi approach, Renew. Energy 105 (2017) 616–624.
[44] E. Khan, K. Ozaltin, D. Spagnuolo, A. Bernal-Ballen, M.V. Piskunov, A. Di Martino, Biodiesel from rapeseed and sunflower oil: effect of the transesterification conditions and oxidation stability, Energies 16 (2023) 657.
[45] C.T. Oloyede, S.O. Jekayinfa, A.O. Alade, O. Ogunkunle, O.T. Laseinde, A. O. Adebayo, A.I. Abdulkareem, G.F. Smaisim, I. Fattah, Synthesis of biobased composite heterogeneous catalyst for biodiesel production using simplex lattice design mixture: optimization process by Taguchi method, Energies 16 (2023) 2197.
[46] V.O. Odude, A.J. Adesina, O.O. Oyetunde, O.O. Adeyemi, N.B. Ishola, A.O. Etim, E. Betiku, Application of agricultural waste-based catalysts to transesterification of esterified palm kernel oil into biodiesel: a case of banana fruit peel versus cocoa pod husk, Waste and Biomass Valorization 10 (2019) 877–888.
[47] A.O. Etim, C.F. Jisieike, T.H. Ibrahim, E. Betiku, Biodiesel and its properties (Chapter 2), in: A. Arumugam (Ed.), Production of Biodiesel from Non-edible Sources, Elsevier, 2022, pp. 39–79.
[48] B. Oladipo, T.V. Ojumu, L.M. Latinwo, E. Betiku, Pawpaw (*Carica papaya*) peel waste as a novel green heterogeneous catalyst for moringa oil methyl esters synthesis: process optimization and kinetic study, Energies 13 (2020) 5834.
[49] A. Saravanan, A.J. Kings, L.M. Miriam, R.R. Isaac, RSM-Based comparative experimental study of sustainable biodiesel synthesis from different 2G feedstocks using magnetic nanocatalyst $CaFe_2O_4$, Environ. Dev. Sustain. 26 (2024) 3097–3126.
[50] S.H. Dhawane, T. Kumar, G. Halder, Biodiesel synthesis from *Hevea brasiliensis* oil employing carbon supported heterogeneous catalyst: optimization by Taguchi method, Renew. Energy 89 (2016) 506–514.
[51] I.U. Khan, Biodiesel production and selected fuel qualities from prospective non-edible oils: *Hevea brasiliensis*, *Madhuca longifolia*, *Azadirachta indica*, and *Gossypium hirsutum*, Int. J. Green Energy 21 (2024) 3054–3071.
[52] B. Nath, P. Kalita, B. Das, S. Basumatary, Highly efficient renewable heterogeneous base catalyst derived from waste *Sesamum indicum* plant for synthesis of biodiesel, Renew. Energy 151 (2020) 295–310.